Optical spectroscopic investigation of segmented *trans*-polyacetylene

G. A. Arbuckle* and A. G. MacDiarmid
Department of Chemistry, University of Pennsylvania, Philadelphia, Pennsylvania 19104

S. Lefrant and T. Verdon
Laboratoire de Physique Cristalline, Institut des Matériaux, Université de Nantes, 2 rue de la Houssinière, 44072 Nantes CEDEX 03, France

E. Mulazzi and G. P. Brivio
Dipartimento di Fisica dell'Università di Milano, via Celoria 16, 20133 Milano, Italy

X. Q. Yang,† H. S. Woo,‡ and D. B. Tanner
Department of Physics, University of Florida, Gainesville, Florida 32611
(Received 20 June 1990)

The optical properties of segmented *trans*-$(CH)_x$ and *trans*-$(CD)_x$ are presented. It is shown from the resonance-Raman-scattering data that a clustering of sp^3 defects occurs upon the introduction of deuterium atoms in *trans*-$(CH)_x$ and hydrogen atoms in *trans*-$(CD)_x$. In view of this effect, the segmented polyacetylene sample still contains long conjugated segments whose electronic properties can account for the almost unchanged optical-band-gap values. The doping-induced infrared bands in different segmented samples are interpreted by considering the perturbation of the dopant on the lattice dynamics of long segments. Also, the dc-conductivity results are discussed in terms of the presence of clusters of sp^3 defects, which can limit both interchain and intrachain transport processes.

I. INTRODUCTION

At the present time, there are a number of methods of producing polyacetylene, $(CH)_x$, samples which can be doped to give high electrical conductivity. These include the original method of Shirakawa and Ikeda (SI),[1] the procedures to obtain either Durham[2] or Assoreni[3] oriented samples of Edwards, Feast, and Bott[2] (EFB) at Durham or of Lugli Pedretti, and Perego[3] (LPP) at Assoreni, the method[4] used by Naarman and Theophilou (NT) and most recently the one developed by Tsukamoto, Takahachi, and Kawasaki (TTK).[5] The maximum conductivity which can be achieved by doping varies substantially among these preparation methods, with both NT and TTK samples showing the highest value (10^5 S/cm). Several factors have been identified as leading to high conductivity: (a) a very low concentration of sp^3 defects, defects that would break the conjugation of the polymer, (b) a high degree of orientation of the chains, (c) a bulk density and morphology which allow a high doping level, (d) the absence of disorder in the samples and (e) a high molecular weight for the polymeric chain.

As previously mentioned,[6] since the conductivity in $(CH)_x$ is controlled by both intermolecular and intramolecular transport processes, it is clear that a small concentration of sp^3-type defects associated with a high degree of chain orientation will affect both mechanisms in a positive way leading to a high bulk conductivity[7,8] [points (a) and (b)]. Also, the bulk density [point (c)], which is related to the synthesis procedure, seems to be a relevant factor in achieving a high conductivity since in EFB-type[9] or LPP-type oriented samples,[3] only a low doping level is obtained. On the contrary, samples prepared in a different way[4,5] can be doped to a high level comparable to that obtained for SI-type[1] polymer films. These factors must be taken into account together. As a matter of fact, although the different segments in the conjugated chain in $(CH)_x$ may be highly conducting, if the activation energy for the transport of charge carriers from one chain to another is high, the macroscopic conductivity is expected to be low. Moreover, extended conjugation is not always necessary for conductivity. For example, a chain of eight $(C_6H_4)N$ units exhibits a conductivity of 1 S/cm upon protonic acid doping,[10] comparable to the conductivity of polyaniline.[11] Here, although the segment conjugation length is short, a good conductivity is obtained. A low-activation-energy interchain process must therefore exist in order to produce the observed bulk conductivity.

Furthermore, iodine doping of different molecular weight $(CH)_x$ samples ranging from 500 to 10^5 daltons (Ref. 12) show no significant increase in conductivity with increasing molecular weight. In fact, the dc conductivity is on the order of 10^2 S/cm for all the different samples. Nevertheless, the analysis of the resonance-Raman-scattering (RRS) spectra of different pristine polymers leads to the conclusion that a significant increase in the concentration of long conjugated segments with respect to the short ones is observed as a function of molecular weight.[13,14] Therefore, it appears that although a delocalized π system is necessary, long conjugated segments are not necessarily needed and they are not alone responsible for bulk electronic conductivity.

A model relationship has been derived[15,16] between

average conjugation length and conductivity, assuming that the individual segments are metallic strands with free electrons. The results of these model calculations agree with some of the experimental data for doped $(CHD_y)_x$ polymers, though the absence of Pauli susceptibility in these samples[17] indicates that the doped segments within the polymer fibrils are not simple metals.

The relationship between the conductivity of polyacetylene and the conjugation length was studied experimentally by Soga and Nakamaru.[18] In their study, partially hydrogenated polyacetylene films $(CH_{1+y})_x$ were doped with iodine from the vapor phase. However, this method of doping is known to result in inhomogeneous doping.[19] Thus, the results—which show that the electrical conductivity depends on the average conjugation length l, where $l \approx 1/y$, when the film is doped—are not completely reliable. In addition, since it is known that the pristine polymer is a rather inhomogeneous material with respect to the conjugation length, it appears difficult to relate in a simple way the experimental values of the conductivity after doping with an average conjugation length.

In order to obtain information on the effects due to the presence of sp^3-type defects on the polymeric chain, many groups have studied the conductivity, the optical properties, and the electrochemical properties of "segmented" *trans*-polyacetylene samples.[17,20–23] Such samples have been called "segmented" from the idea that an sp^3 defect provides an essentially complete interruption of the conjugation length.[24]

A series of studies[22] of "segmented" $(CH)_x$ doped with the usual oxidizing agents such as AsF_5 or I_2, shows that conductivities of 1 S/cm can be obtained for samples of $(CHD_{0.16})_x$, when doped to a maximum level, suggesting relatively strong intrachain and/or interchain transport processes. A stronger temperature dependence of the conductivity was observed in the "segmented" samples as compared to *trans*-$(CH)_x$ doped to the same level.[22] This observation supports the viewpoint that in the "segmented" samples, the charges in the polymeric chain are more localized due to the insertion of the sp^3 units.

In this paper we present an extensive study of the optical properties of the $(CH)_x$ and $(CD)_x$ films segmented by the introduction of the sp^3 defects in a controlled way through the insertion of deuterium and of hydrogen atoms, respectively, in the samples. The concentration of these defects ranges from 0.0 to 0.3 in $(CH)_x$ and from 0.0 to 0.27 in $(CD)_x$. The purpose of this work is to study how the optical properties are changed by sp^3 defects. The present study provides information on the way the sp^3 defects are distributed along the chains from the following: the change in the band gap, the broadening, and the shift of the uv-visible absorption bands, and the broadening and shift of the resonant Raman bands with respect to the pristine polymer. Also, the modifications which occur upon doping on the infrared absorption of samples with various sp^3 defect concentrations can give additional information on this matter.

The synthesis and the preparation of the segmented $(CH)_x$ and $(CD)_x$ are reported in Sec. II. In Sec. III the optical properties of such samples are described, i.e., the uv-visible absorption, the infrared absorption together with the experimental and theoretical analysis of the resonant-Raman-scattering data. Also, infrared and near-infrared spectra of the iodine-doped segments samples are given. In Sec. IV the discussion and the conclusion are given.

II. SYNTHESIS AND PREPARATION

All $(CH)_x$ or $(CD)_x$ films used in the present study were prepared from the *cis* isomer synthesized at $-78\,^{\circ}C$ following the SI procedure.[1] Thermal treatment at $\approx 160\,^{\circ}C$ for 1 h was performed to achieve the complete isomerization to the *trans* form.

The general method of preparation of *trans*-$(CHD_y)_x$ or *trans*-$(CDH_y)_x$ has been described elsewhere.[21,22] We recall here that the procedure is based on the method of Pron[25] and Kletter.[26] They showed, in particular, that samples of $(CH)_x$, upon heavy *n*-type doping with sodium naphthalide/tetrahydrofuran (THF) solutions, result in metallic *n*-type doped films of composition $(CHNa_y)_x$. Subsequent exposure of these films to CH_3OH, CH_3OD, H_2O, or D_2O resulted in hydrogenation and deuteration, respectively. Soga *et al.*[18] have shown similar results upon heavy doping of polyacetylene with potassium naphthalide/THF solutions, followed by a treatment of the potassium-doped films with methanol or deuterated methanol.

The conversion of $(CH)_x$ to $(CHD_y)_x$ is achieved via reaction (1) which is carried out in THF solution:

$$(CH)_x + xyNa^+(C_{10}H_8)^- \rightarrow [Na_y{}^+(CH)^{y-}]_x + xyC_{10}H_8 \ . \tag{1}$$

The $[Na_y{}^+(CH)^{y-}]_x$ film, after washing with THF, is permitted to react with CH_3OD, viz.,

$$[Na_y{}^+(CH)^{y-}]_x + xyCH_3OD \rightarrow [CHD]_x + xyCH_3ONa \ . \tag{2}$$

A very accurate measurement of the value of y may be made by titration of the methanol solution resulting from the reaction shown in Eq. (2) with HCl. The same procedure can be used for synthesizing $(CDH_y)_x$ by using $(CD)_x$ instead of $(CH)_x$ in the above reactions. This method produces films with $y \approx 15\%$. Films with a higher level of partial deuteration ($y = 0.30$) and hydrogenation ($y = 0.27$), respectively, were prepared by repeating the procedure using $(CHD_y)_x$ or $(CDH_y)_x$ instead of $(CH)_x$. In this way, hydrogen or deuterium is incorporated in the samples and sp^3-hybridized defects are thereby introduced in a controlled manner.

This type of defect is expected to break the conjugation significantly leading to "segmented" polyacetylene samples. Specific properties such as electronic optical absorption, vibrational infrared absorption, RRS and EPR can be studied as a function of the sp^3 defects concentration in undoped samples such as those synthesized above or after doping them with iodine, AsF_5 or $HClO_4$ (Refs. 20 and 22).

III. OPTICAL PROPERTIES

A. uv-visible absorption

The optical measurements were made either as transmission or reflection, depending on whether the samples were transparent or not. For the sample thicknesses used (≈ 50 μm) and doping levels achieved ($<2\%$), we were able to make transmission measurements below about 3000 cm^{-1}, but were only able to make reflection measurements at higher frequencies. The transmittance T was analyzed to give the absorption coefficient, defined as $\alpha=(1/d)\ln T$, where d is the thickness of the $(CH)_x$ film. The reflectance was analyzed by the Kramers-Kronig methods to give the phase shift on reflection, after which the optical constants were calculated. The absorption coefficient is then $\alpha=2(\omega/c)\kappa$, where κ is the imaginary part of the complex refractive index and ω the frequency. On account of inhomogenities and rough surfaces, it is expected that the transmission is the quantitatively more accurate method.

The optical-absorption spectra of *trans*-$(CH)_x$ and *trans*-$(CHD_{0.16})_x$ recorded at room temperature[20] are presented in Fig. 1. The maximum absorption which occurs at ≈ 2 eV in *trans*-$(CH)_x$ is slightly shifted to higher energies (≈ 2.2 eV) for *trans*-$(CHD_{0.16})_x$. Also, the Kramers-Kronig analysis of reflectance spectra of $(CHD_y)_x$, with y ranging from 0.0 to 0.16 showed a similar shift in the absorption peak, along with an overall reduction of the intensity in the visible region.[20,22]

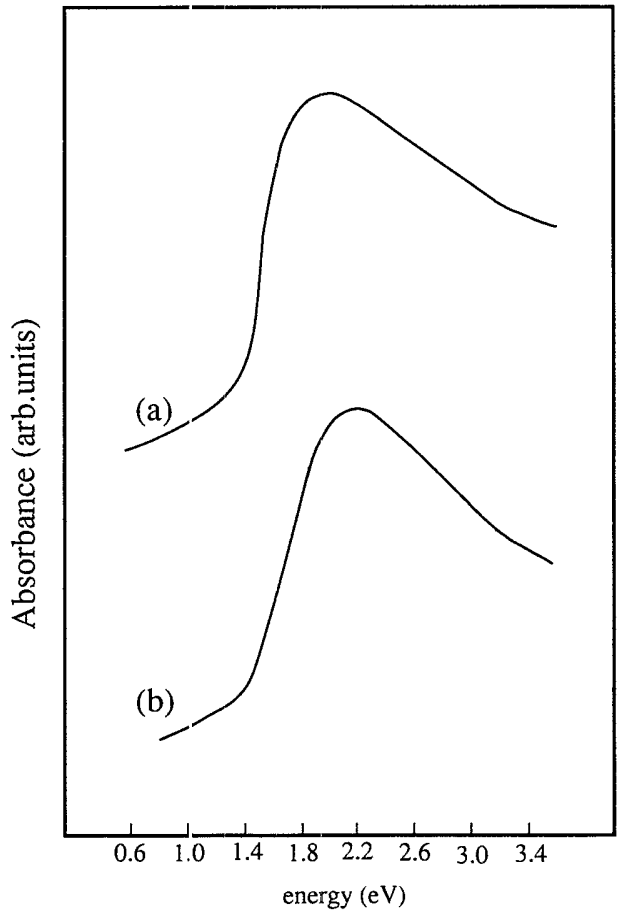

FIG. 1. Optical absorption of a thin film of (a) *trans*-$(CH)_x$; (b) *trans*-$(CHD_{0.16})_x$.

B. Infrared spectra

Infrared spectra of segmented *trans*-$(CH)_x$ and *trans*-$(CD)_x$ are shown in Fig. 2 together with those of the pristine polymer for comparison. The spectra of *trans*-$(CHD_{0.16})_x$ and *trans*-$(CHD_{0.30})_x$ strongly resembles that of *trans*-$(CH)_x$ whose main bands have been assigned previously.[1] The two main differences are the two bands at 2905 and 2148 cm^{-1}, which are due to C—H and C—D stretching vibrations, respectively, of sp^3 hydridized carbon. The intensity of these two modes increases gradually with increasing values of y. This result confirms the composition of the deuterated and hydrogenated polymers. The absence of absorbance around 1400 and 850 cm^{-1}, where the doping-induced bands in *trans*-(CH_x) occur, indicate that the n-type dopant was removed in treatment with the alcohol during the synthesis of *trans*-$(CHD_y)_x$ and $(CDH_y)_x$.

The spectra of $(CDH_{0.15})_x$ and $(CDH_{0.27})_x$ are also very similar to that of *trans*-$(CD)_x$ for which the band assignments have been published.[1] Again, new stretching modes from sp^3-hybridized carbons are observed at 2899 and 2152 cm^{-1} whose intensity increases with increasing values of y.

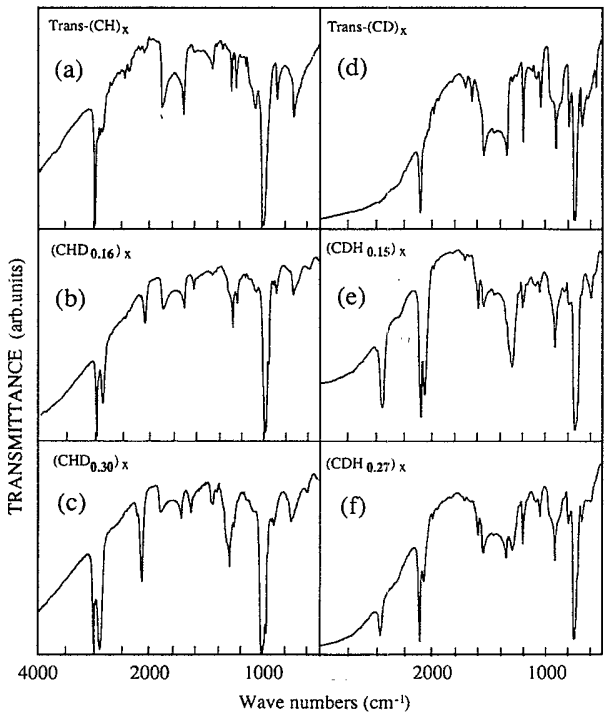

FIG. 2. Fourier-transform infrared spectra of (a) *trans*-$(CH)_x$; (b) *trans*-$(CHD_{0.16})_x$; (c) *trans*-$(CHD_{0.30})_x$; (d) *trans*-$(CD)_x$; (e) *trans*-$(CDH_{0.15})_x$; (f) *trans*-$(CDH_{0.27})_x$.

C. Resonance Raman-scattering spectra

1. Experimental

RRS spectra of *trans*-$(CHD_y)_x$ for $y=0.0$, 0.069, 0.11, and 0.16 have been reported previously[27,28] for the two excitation wavelengths $\lambda_L=676.4$ and 457.9 nm. Here in Fig. 3 we show additional RRS spectra for segmented samples with $y=0.16$ and 0.28, with excitation at $\lambda_L=647.1$ 457.9, and 351.1 nm.

In Fig. 4 we present the spectra of segmented *trans*-$(CDH_y)_x$ for $y=0.27$ for $\lambda_L=676.4$, 600, 514.5, and 351.1 nm. Here, we show only RRS spectra of a particular sample since the comparison between spectra of $(CDH_y)_x$ films for different y values have already been presented.[28]

Let us notice that in both cases, going from $y=0.0$ 0.16 (in $CHD_y)_x$ or to 0.15 (in $CDH_y)_x$, some modifications in the band shapes and peak positions occur. From the analysis of the spectra, which is reported below, it is shown that these changes are well explained in terms of a shortening of the length of the conjugated segments. On the other hand, as already mentioned,[27,28] almost no differences are seen in the RRS spectra going from $y=0.16$ to 0.28 and from $y=0.15$ to 0.27, respectively, for all the laser wavelengths. This behavior was also reported by Furukawa *et al.*[29] in hydrogenated $(CH)_x$ samples. These results suggest that no further shortening has occurred after achievement of the higher sp^3 defect concentration (0.28 and 0.27, respectively). We note in addition that the first chemical treatment (*n*-type doping and compensation) leads to a maximum $y\approx0.16$ and a second complete identical treatment is needed to obtain the $y\approx0.27$–0.28 sample as mentioned above. Furthermore, in the segmented polyacetylene samples, slight differences in the band profiles of the RRS spectra were observed after aging (1 or 2 months) as determined by repeating RRS experiments.

2. Theoretical analysis

The different features of the Raman spectra given above can be analyzed and interpreted in terms of the model presented in detail.[30,31] We recall here that the Raman band shapes are evaluated in that model by considering the electronic transitions and the Raman-active vibrational frequencies and the related couplings in the electronic excited states between the electrons and the vibrations of the conjugated segments of different length. All the different contributions in the Raman-scattering cross sections are weighted by using a bimodal distribution of conjugated segments. Following this model, it

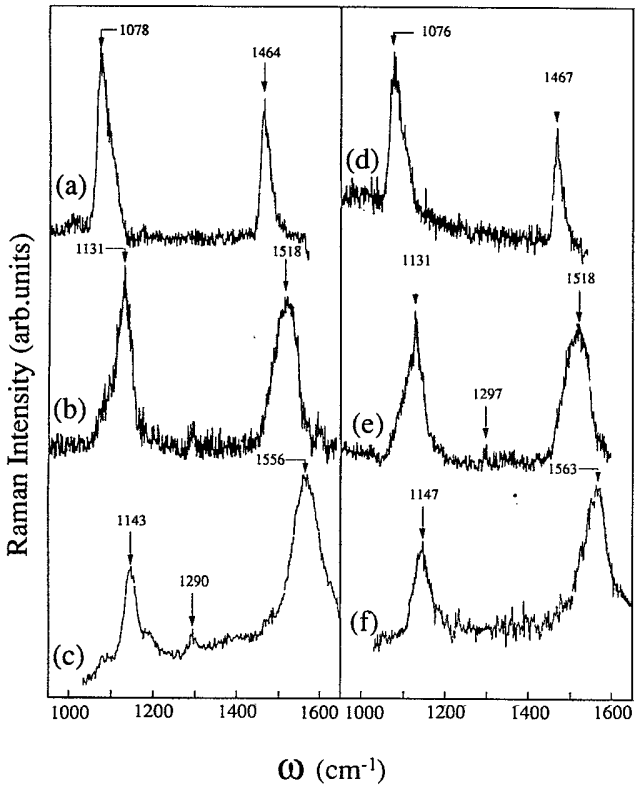

FIG. 3. Raman spectra at $T=300$ K of $(CHD_{0.16})_x$, (a) $\lambda_L=647.1$ nm; (b) $\lambda_L=457.9$ nm; (c) $\lambda_L=351.1$ nm; $(CHD_{0.28})_x$, (d) $\lambda_L=647.1$ nm; (e) $\lambda_L=457.9$ nm; (f) $\lambda_L=351.1$ nm.

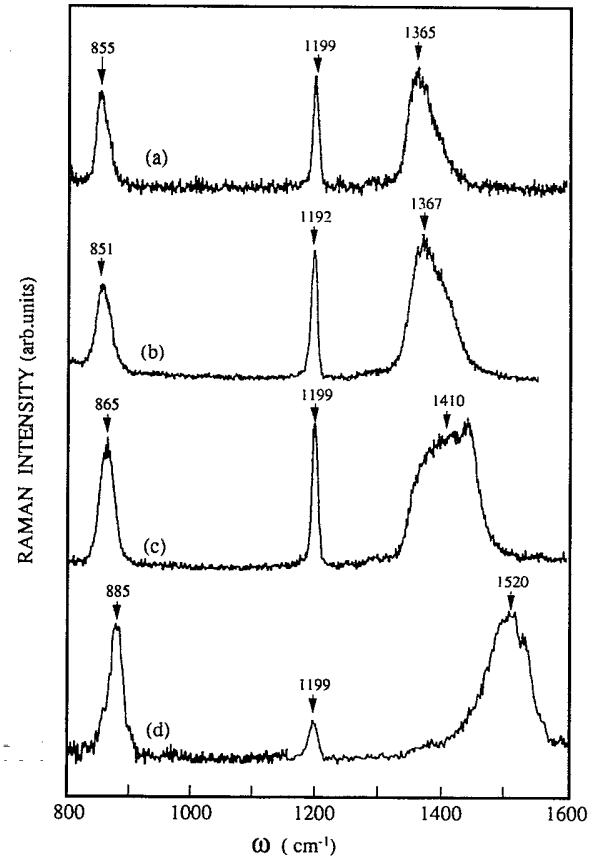

FIG. 4. Raman spectra of $(CDH_{0.27})_x$ at $T=300$ K; (a) $\lambda_L=676$ nm; (b) $\lambda_L=600$ nm; (c) $\lambda_L=514.5$ nm; (d) $\lambda_L=351.1$ nm.

TABLE I. Parameters of the two distributions for the RRS spectra of $(CHD_y)_x$.

Sample	N_1	N_2	σ_1	σ_2	G
$(CH)_x$	60	20	30	7	0.55
$(CHD_{0.069})_x$	40	15	20	7	0.5
$(CHD_{0.11})_x$	40	15	20	7	0.4
$(CHD_{0.17})_x$	30	10	15	5	0.4

was shown that the quality of the sample, in terms of the percentage of long conjugated segments with respect to that of the short ones, can be determined.[32] As an example, a Shirakawa-type sample of good quality is described with the bimodal distribution centered on segments of 100 double bonds (N) with a weight $G=0.75$ with respect to the short ones whose distribution is centered on $N=15$ with a relative weight of 0.25. A little higher value for the long segment distribution ($G=0.8$) is found when the Raman-scattering bands are analyzed for the high molecular weight samples.[12,13]

The $(CHD_y)_x$ RRS spectra are interpreted by the bimodal distribution model presented before and related parameters are collected in Table I. In Table II the parameters obtained from the analysis of the RRS spectra for the freshly prepared $(CDH_y)_x$ samples (A) are given together with those of the two-month-old samples (B). Note that the RRS spectra given in Fig. 4 have been recorded from the two-month old samples. From Tables I and II, we notice that by the addition of hydrogen or deuterium atoms, a significant decrease in the conjugated length of the segments is observed. This effect can be deduced from the downwards shift of the peaks of the two distributions. In addition, the G coefficient, which weights the long segment distribution with respect to the short segment one, decreases as the concentration of the sp^3 defects increases. Note that the long segment distribution has still a relatively large weight although the concentration y is rather high for $(CHD_{0.17})_x$ and $(CDH_{0.27})_x$. These calculations, which give evidence for the predominance of short segments in the film with a high concentration of additional sp^3 (CDH) units, are in agreement with the optical-absorption spectra which show peaks shifted to the violet as previously reported[20,33] and in Fig. 1. It is worthwhile noting that by aging in a sealed evacuated sample tube, further modifications have been observed in the RRS spectra.

TABLE II. Parameters of the two distributions for the RRS spectra of $(CDH_y)_x$.

	Sample	N_1	N_2	σ_1	σ_2	G
A	$(CD)_x$	35	17	15	5	0.45
	$(CDH_{0.15})_x$	30	10	15	5	0.42
	$(CDH_{0.27})_x$	30	7	15	3	0.40
B	$(CD)_x$	50	17	20	5	0.45
	$(CDH_{0.15})_x$	40	10	15	5	0.45
	$(CDH_{0.27})_x$	40	10	15	5	0.40

These parameters are also shown in Table II. In particular, slightly longer segments are present in samples B and the parameters related to these samples do not change by increasing the y concentration from 0.15 to 0.27, contrary to what is found in samples A.

D. INFRARED SPECTRA OF DOPED SEGMENTED SAMPLES

1. Experimental

In Fig. 5 we show the infrared spectra of $[CHD_y(I_3)_z]_x$ and $[CDH_y(I_3)_z]_x$ respectively for $y=0.15-0.16$. The doping concentration z was determined to be 0.007 for segmented $(CH)_x$ and 0.0256 for segmented $(CD)_x$. In the figure, we show for comparison ir spectra of undoped samples. The doping-induced bands in segmented $(CH)_x$ [Fig. 5(a)] appear at 880, 1290, and 1400 cm^{-1} while in segmented $(CD)_x$, they peak at 740 and 1140 cm^{-1} [Fig. 5(b)] respectively. In segmented $(CD)_x$, an additional band reported before[34] at 1240 cm^{-1} is not resolved in this spectrum. We note that all other features in the spectra are rather similar to those reported in the literature[34,35] for ordinary doped *trans*-polyacetylene. This is an indication that the frequencies of the doping induced

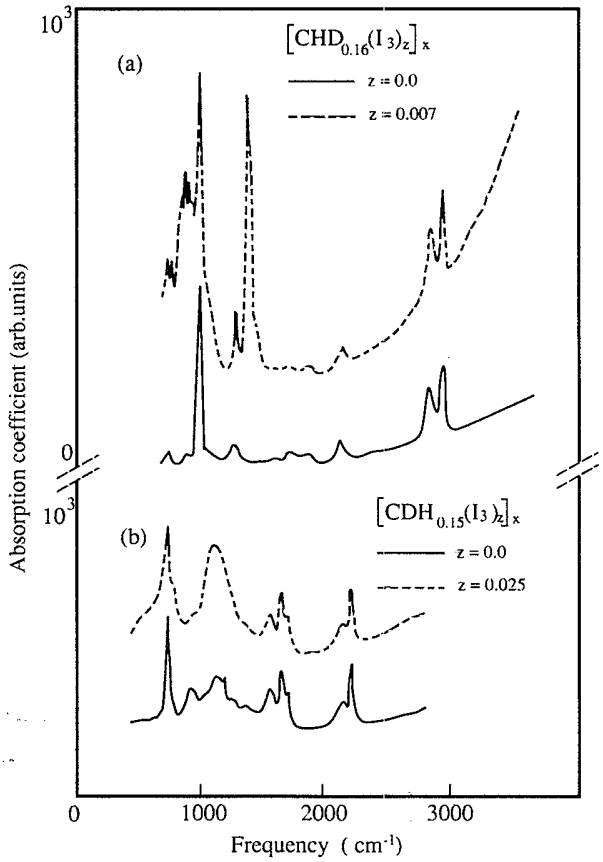

FIG. 5. Infrared spectra of doped segmented samples: (a) $[CHD_{0.16}(I_3)_z]_x$ for $z=0.0$(——) and $z=0.007$(— — —); (b) $[CDH_{0.15}(I_3)_z]_x$ for $z=0.0$(——) and $z=0.0256$(— — —).

ir modes are very little changed in doped segmented samples compared with pristine films. In contrast, the intensities of all the bands are decreased as reported[20] in the case of doped segmented $(CH)_x$ compared with the pristine polymer doped to the same level. A similar behavior is observed in doped segmented $(CD)_x$ as illustrated in Fig. 6 in which we show the integrated oscillator strength of the 1140-cm^{-1} band in different samples as a function of the dopant concentration. It should be noted that this effect is dependent upon the sp^3 concentration level, y, as shown by the further intensity decrease observed in $(CDH_{0.27})_x$ compared with $(CDH_{0.15})_x$. This point will be discussed later, since from the RRS spectra, no significant difference has been recorded for the two samples mentioned above.

2. *Theoretical interpretation*

The doping-induced infrared bands whose peak positions are reported above can be explained by following the perturbed Green-function method applied to the *trans*-polyacetylene as previously reported.[36,37] From the values of the frequencies of the band peaks which do not change in the different segmented samples (y ranging from 0.0 to 0.16 having the same z dopant concentration value), it appears that mainly the long and intermediate segments are more easily doped. Then the doping-induced modes are due to the perturbation induced by the dopant on the lattice dynamics of these kind of segments, just as in the case of ordinary $(CH)_x$. Short segments, whose concentration is increased at larger y values, do not appear to contribute to the position of the peaks of the doping induced bands in this particular case. This result is different from that reported previously[35] where a shift of the peaks of the doping-induced bands towards higher frequencies is observed as function of the content of short segments within the samples. Thus, it appears that the short segments in the segmented polyacetylene samples are too short to permit good charge delocalization and to accommodate dopants. We recall that from the Raman data analysis of the segmented samples reported in Table I and II, the short segment distribution is centered on $N=10$.

Taking into account the lattice dynamics of long segments, the different frequencies of the band peaks can be found at 850, 1280, and 1400 cm^{-1} for a change of the force constant $\Lambda \approx 30\times10^6$ cm^{-2} in *trans*-$(CHD_y)_x$ for $y=0.16$ and at 700, 1140, and 1240 cm^{-1} in *trans*-$(CDH_y)_x$ for $y=0.15$, with the same value of Λ. The contribution of the intermediate segments (N ranging from 25 to 15) can introduce a shift in the position of these peaks towards higher frequencies.

E. Near-infrared spectra of doped segmented samples

We show in Fig. 7 the near-infrared absorption spectra, determined by the Kramers-Kronig analysis of reflectance, of doped segmented $(CH)_x$ and $(CD)_x$. In Fig. 7(a), spectra of $[CHD_{0.16}(I_3)_z]_x$ are shown for two different z values as indicated. Notice that the intensity of the midgap band ($\approx$6000 cm^{-1}) increases with the z value, while that of the main band in the visible region decreases. Also, a shift of the peak of this latter band towards higher frequencies is observed with increasing z

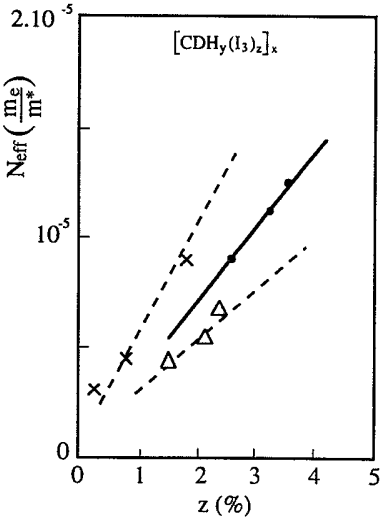

FIG. 6. Integrated oscillator strength of the 1140 cm^{-1} band in $[CDH_y(I_3)_z]_x$ for $y=0.0(\times)$; $y=0.15(\bullet)$; $y=0.27(\triangle)$ as a function of the dopant concentration.

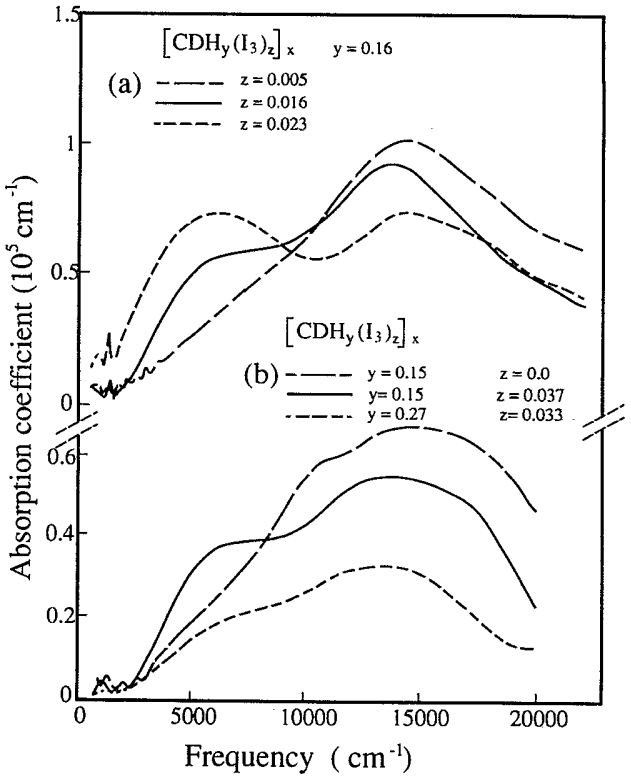

FIG. 7. Near-infrared spectra of doped segmented polyacetylene: (a) $[CHD_{0.16}(I_3)_z]_x$, $z=0.005$(– – –); $z=0.016$(——); $z=0.023$(— — —); (b) $[CDH_y(I_3)_z]_x$, $y=0.15$, $z=0.000$(– – –); $y=0.15$, $z=0.037$(——); $y=0.27$, $z=0.033$(— — —).

values. Similar behavior is observed for $[CDH_y(I_3)_z]_x$. In addition, as shown in Fig. 7(b), for doped segmented $(CD)_x$, the features of the spectra of the samples, with $y=0.15$ and 0.27 and almost the same z value, do not change as function of the sp^3 concentration level, the only difference being the intensity of the bands which decreases with increasing y values. This is an important point to be discussed later since, as noticed before, the RRS spectra of the undoped samples with the above reported sp^3 concentration levels do not show significant differences.

IV. DISCUSSION AND CONCLUSION

In this paper we have reported experimental optical data of segmented *trans*-polyacetylene, $(CHD_y)_x$ and $(CDH_y)_x$, together with the theoretical interpretation of the Raman data and the doping-induced infrared bands.

In principle, deuteration or hydrogenation of polyacetylene might be expected to result in the controlled increase in the band gap of the polymer. However, the results show that the optical absorption band gap is not significantly modified even for sp^3 concentration level y as high as 0.3.

Another important point in this study was to investigate the relationship between conjugation length and conductivity after doping, and, in particular, the role of the presence of sp^3 defects in changing the interchain and intrachain transport processes of the charge carriers. The measurements reported previously[22] show that by doping either with $HClO_4$ or with AsF_5 (10%) (vapor phase), the dc conductivity values are for $y=0.0$ approximately 250–400 S/cm, while for $y=0.30$ of the order of 10^{-2} S/cm. It is observed that a real decrease in conductivity occurs by increasing the concentration of sp^3 defects in the samples. On the other hand, if one considers the length of the conjugation segments, as derived from an homogeneous distribution of defects,[18] the dc conductivity values cannot be accounted for. These two points, i.e., the results of the optical band gap and the dc conductivity, can be somewhat clarified by considering the results of analysis of the RRS spectra of segmented $(CH)_x$ and $(CD)_x$. They suggest (see Sec. III) that a clustering of sp^3 defects occurs during the segmentation process. As previously proposed,[27] a bimodal distribution of conjugation segments is considered in the calculation in order to account for the evolution of the Raman spectra of samples with different concentration of sp^3 defects. As a consequence, long segments are still present in the sample, even at high sp^3 defects concentration, together with conjugated segments whose length has been shortened compared with that in the pristine polymer. The effect of clustering which was proposed first for segmented $(CH)_x$ (Ref. 27) has been confirmed in segmented $(CD)_x$ (Ref. 28). A strong support to these results has been given by the calculations previously reported[38,39] where a bimodal distribution of conjugated segments is also proposed in order to account for the clustering effect.

In view of the above-reported results, it is possible to explain the experimental data on the band gap of polyacetylene samples with different sp^3 concentrations. Since long segments still exist for all the y concentration levels considered, the band gap is not expected to change compared with the value in pristine films.

Moreover, following the analysis of the Raman data, it is possible to explain the shift of the absorption optical band peak towards higher energies and the intensity decrease of the overall band as a function of sp^3 concentration. In fact, the increase of the number of short segments with respect to that of the long ones in the different samples account for both effects, since electronic transitions of the short segments occur at higher energies and the related transition dipole moments decrease as already shown.[30] Again these results on the length of conjugated segments are important to explain the dc conductivity values, which are not negligible (10^{-2} S/cm) in doped samples with a concentration of sp^3 defects as high as 30%. A careful analysis of the results of the dc conductivity of the doped segmented samples reveals that the dc conductivity decreases by increasing the concentration of sp^3 defects in the samples.[6,22] Thus, although the addition of sp^3 defects, which seems to form clusters on the chain, does not change the Raman band shapes when y varies from 0.16 to 0.30 (see Sec. III), the conductivity is affected dramatically.

Furthermore, as we have discussed before,[6] these results offer a further indication that the length of the conjugated segments in the polymeric chains, together with the nature of the defects which limits this length, seem to play an important role in the intrachain and interchain carrier mobility. Then, these data seem to indicate that sp^3 defects tend to limit the interchain and intrachain transport processes and that the clustering of these type of defects is even more efficient in inhibiting these processes.

It should be noted that the maximum concentration of iodine dopant which can be introduced in the segmented samples is 3%, which is only one-half of the usual dopant concentration in pristine samples.

Moreover, the intensity of the infrared bands in the segmented samples decreases with increasing y values, as indicated[20] and also reported in Sec. III D while their peak position and their band shapes are almost unchanged. Also, with increasing y values, the near-infrared optical bands in the doped segmented samples display a decreasing intensity (see Sec. III E). It has been shown[39] that, if two I_3^- ions have to be accommodated on the conjugated segments (even number of sites), a minimum distance of 20–25 sites between sp^3 defects should be required to generate such a pair. This would be a possible explanation for the fact that the maximum iodine doping concentration allowed in the sample is only 3%. In fact, from the Raman data analysis (Sec. III C), we found that the short segment distribution is centered at $N\approx 10$ (i.e., 20 sites) for $y=0.17$ and 0.30. The capability of doping the conjugated segments in such samples decreases since on one hand, the short segments are too short to accommodate two I_3^- ions and on the other hand, the concentration of long and intermediate segments decreases with increasing y value. This interpretation is further corroborated by the decrease of the intensities of the ir and near-ir bands without any shift of their

peak positions (see also Sec. III D).

Finally, it should be noted that all the data recorded from doped films are obtained in segmented samples doped in vapor phase. It is well known[22] that this type of procedure leads to a very inhomogeneous doping of the polymer. This can be an additional factor responsible for the decrease of the intensities of both ir and near-ir bands. In addition, the systems doped in such a way are disordered and it may be rather unreliable to compare experimental data obtained for the same z dopant concentration from different segmented samples.

The optical results are in agreement with conclusions obtained from electrochemical n-type doping studies of segmented polyacetylene $(CHD_y)_x$ (Ref. 21). Since the injection potentials for n-type doping of *trans*-$(CH)_x$ and *trans*-$(CHD_{0.15})_x$ were found to be essentially identical, it was concluded that long conjugated segments, which are doped preferentially, are present in both $(CH)_x$ and $(CHD_{0.15})_x$. Changes in open circuit potential, V_{oc}, as a function of time for *trans*-$(CH)_x$ and *trans*-$(CHD_{0.15})_x$ indicated that the diffusion is significantly slower in *trans*-$(CHD_{0.15})_x$ than in $(CH)_x$, indicating that the negative charge is more localized, due to the sp^3-hybridized defects.

The clustering of sp^3-hybridized defects has also been alluded to in order to explain the two orders-of-magnitude reduction in the intrachain diffusion of solitons in *trans*-$(CHD_{0.15})_x$ as determined by EPR and NMR studies.[23] The intrachain diffusion rate is reported to be larger than the interchain diffusion rate in *trans*-$(CHD_{0.15})_x$, suggesting that three-dimensional behavior becomes increasingly important in segmented polyacetylene.

In conclusion, the results of the present study are consistent with the above observations. In particular, we have shown that, upon introducing sp^3 defects in *trans*-$(CH)_x$ or trans-$(CD)_x$ polymer films, a clustering of defects occurs as evidenced from the Raman data analysis. This agrees well with the almost unchanged band gap in different segmented samples. Also, the clustering explains the nonnegligible dc conductivity in doped samples with high sp^3 defects concentration and it is responsible for the decreasing values of the inter and intrachain transport processes of the change carriers in the samples with increasing y values. This is an important result in order to give some enlights on which parameters are important to be controlled in obtaining high-conductivity $(CH)_x$ samples.

ACKNOWLEDGMENTS

One of us (E.M.) wants to thank partial support from a bilateral program CNR Italy–France. Work at the University of Florida was supported by DARPA-URI-N00014-86-A0224. Work at the University of Pennsylvania was supported by the U.S. National Science Foundation (Grant No. DMR-86-15475). The authors want to thank Professor A. J. Epstein, the Ohio State University, for very helpful discussions. J. C. Ricquier, Laboratoire de Physique Cristalline of the University of Nantes, is greatly acknowledged for his help in the preparation of the manuscript. The Institut des Matériaux is "Unité Mixte de Recherche Centre National de la Recherche Scientifique, Université de Nantes."

*Present address: Rutgers University, Department of Chemistry, Camden College of Arts and Sciences, Camden, NJ 08102.

†Present address: Brookhaven National Laboratory, Upton, NY 11973.

‡Present address: Cavendish Laboratory, Madingley Road, Cambridge CB3 OHE, U.K.

[1]H. Shirakawa and S. Ikeda, Polym. J. **2**, 231 (1971).

[2]J. H. Edwards, W. J. Feast, and D. C. Bott, Polym. **25**, 395 (1984).

[3]G. Lugli, V. Pedretti, and G. Perego, Mol. Cryst. Liq. Cryst. **117**, 43 (1985).

[4]H. Naarman and N. Theophilou, Synth. Metals **22**, 1 (1987).

[5]J. Tsukamoto, A. Takahashi, and K. Kawasaki, Jpn. J. Appl. Phys. **29**, 125 (1990).

[6]S. Lefrant, T. Verdon, and E. Mulazzi, Synth. Metals, **35**, 123 (1990).

[7]Th. Schimmel, G. Denninger, W. Riess, J. Voit, M. Schoerer, W. Schoepe, and H. Naarman, Synth. Metals D **28**, 11 (1989).

[8]N. Theophilou, D. B. Swanson, A. G. MacDiarmid, A. Chakraborty, H. H. S. Javadi, R. P. Mccall, S. P. Treat, F. Zuo, and A. J. Epstein, Synth. Metals D **28**, 35 (1989).

[9]G. Leising, Phys. Rev. B **38**, 10313 (1988).

[10]F. L. Lu, F. Wudl, M. Nowak, and A. J. Heeger, J. Am. Chem. Soc. **108**, 8311 (1986).

[11]A. G. MacDiarmid, J. C. Chiang, M. Halpern, W. S. Huang, S. L. Mu, N. L. D. Somasiri, N. Wu, and S. I. Yaniger, Mol. Cryst. Liq. Cryst. **121**, 173 (1985).

[12]M. A. Schen, Ph.D. thesis, University of Amherst, 1985. Available from the University Microfilms International, 300 N. Zeeb Road, Ann Arbor, Michigan 48106.

[13]M. A. Schen, J. C. W. Chien, E. Perrin, S. Lefrant, and E. Mulazzi, J. Chem. Phys. **89**, 7615 (1988).

[14]M. A. Schen, S. Lefrant, E. Perrin, J. C. W. Chien, and E. Mulazzi, Synth. Metals D **28**, 287 (1989).

[15]R. H. Baughman and L. W. Schacklette, Synth. Metals **17**, 173 (1987).

[16]R. H. Baughman and L. W. Shacklette, Phys. Rev. B **39**, 5872 (1989).

[17]F. Zuo, A. J. Epstein, X. Q. Yang, D. B. Tanner, G. A. Arbuckle, and A. G. MacDiarmid, Synth. Metals **17**, 433 (1987).

[18]K. Soga and M. Nakamaru, J. Chem. Soc., Chem. Commun. 1495 (1983).

[19]A. J. Epstein, H. Rommelmann, M. A. Druy, A. J. Heeger, and A. G. MacDiarmid, Solid State Commun. **38**, 683 (1981).

[20]X. Q. Yang, D. B. Tanner, G. A. Arbuckle, A. G. MacDiarmid, and A. J. Epstein, Synth. Metals **17**, 277 (1987).

[21]M. X. Wan, G. A. Arbuckle, A. G. MacDiarmid, and A. J. Epstein, Synth. Metals **24**, 283 (1988).

[22]G. A. Arbuckle, Ph.D. thesis, University of Pennsylvania 1987. Available from the University Microfilms International, 300 N. Zeeb Road, Ann Arbor, Michigan 48106.

[23]Y. Cao, R. Gaines, A. J. Epstein, G. A. Arbuckle, and A. G. MacDiarmid, Phys. Rev. B **40**, 3176 (1989).

[24]J. Kürti and H. Kuzmany, in *Electronic Properties of Conjugated Polymers, Vol. 76 of Springer Series in Solid State Sciences,* edited by H. Kuzmany, M. Mehring, and S. Roth (Springer-Verlag, Berlin, 1987), p. 43.

[25]A. Pron, Ph.D thesis, Univeristy of Pennsylvania, 1980. Available from the University Microfilms International, 300 N. Zeeb Road, Ann Arbor, Michigan 48106.

[26]M. J. Kletter, Ph.D. thesis, University of Pennsylvania, 1983. Available from the University Microfilms International, 300 N. Zeeb Road, Ann Arbor, Michigan 48106; S. I. Yaniger, M. J. Kletter, and A. G. MacDiarmid, Polym. Prepr. **25**, 264 (1984).

[27]S. Lefrant, G. A. Arbuckle, E. Faulques, E. Perrin, A. Pron and E. Mulazzi, in *Electronics Properties of Conjugated Polymers,* Vol. 76 of *Springer Series in Solid State Sciences,* edited by H. Kuzmany, M. Mehring, and S. Roth (Springer-Verlag, Berlin 1987), p. 54.

[28]E. Mulazzi, G. P. Brivio, S. Lefrant, E. Perrin, G. A. Arbuckle, and A. G. MacDiarmid, Synth. Metals **28**, D309 (1989).

[29]Y., Furukawa, T. Arakawa, H. Takeuchi, I. Harada, and H. Shirakawa, J. Chem. Phys. **81**, 2907 (1984).

[30]G. P. Brivio and E. Mulazzi, Phys. Rev. B **30**, 876 (1984).

[31]R. Tizani, G. P. Brivio, and E. Mulazzi, Phys Rev. B **31**, 4015 (1985).

[32]S. Lefrant, E. Faulques, G. P. Brivio, and E. Mulazzi, Solid State Commun. **53**, 583 (1985).

[33]H. S. Woo, F. Gao, D. B. Tanner, G. A. Arbuckle, and A. G. MacDiarmid, Bull. Am. Phys. Soc. **33**, 491 (1988).

[34]B. François, M. Bernard, and J. André, J. Chem. Phys. **75**, 4143 (1981).

[35]P. Piaggio, G. Dellepiane, E. Mulazzi, and R. Tubino, Polymer **28**, 563 (1987).

[36]G. P. Brivio and E. Mulazzi, Solid State Commun. **60**, 203 (1986).

[37]G. P. Brivio and E. Mulazzi, Synth. Metals, **17**, 273 (1987).

[38]J. L. Brédas, J. M. Toussaint, G. Hennico, J. M. André, A. J. Epstein, and A. G. MacDiarmid, in *Electronic Properties of Conjugated Polymers* (Ref. 24), p. 48.

[39]S. Jeyadev and E. M. Conwell, Phys. Rev. B **37**, 8262 (1988).